Proceedings of the 2020 Design of Medical Devices Conference
DMD2020
April 6, 7-9, 2020, Minneapolis, MN, USA

DMD2020-9003

NUMERICAL MODELING OF VASCULAR STRESSES DURING LEAD EXTRACTION: SUBCLAVIAN VS. FEMORAL

Mostafa Toloui (PhD)[1], Mark Marshall[2], Pierce Vatterott (MD)[3]
1: Coronary & Structural Heart division, Medtronic
2: Cardiac Rhythm & Heart Failure division, Medtronic
3: United Heart & Vascular Clinic, St. Paul, MN

Peter Zhang[2], Ryan Lahm[2], Thomas Lulic[2] and Megan Harris[2]
2: Cardiac Rhythm & Heart Failure division, Medtronic

ABSTRACT

Transvenous lead extraction is a critical and growing technique used to treat patients with chronically implanted pacemakers and defibrillators. This procedure is commonly executed via the subclavian vein or the femoral vein. Some physicians' experiences indicate that the femoral approach results in fewer vascular tears. This study is aimed to present a physics-based comparative assessment of intravenous mechanical stresses for chronic lead management between the two approaches. Finite Element (FE) modeling is employed to quantify the vascular stress distributions. A full 3-D model including veins, heart, fibrotic scar regions and the lead was created to simulate the different lead extraction methods. Results: (1) highest stresses are generally in the vicinity of SVC lead attachments; (2) femoral approach results in a ~uniform distribution of stress over the scar while the subclavian approach leads to patches of concentrated high stress; (3) 2-3 times higher maximum vascular stress during subclavian; (4) insignificant maximum stress at the apex for both; (5) inverse variation of stress levels with: (i) branch-to-scar distance for SVC method; and (ii)vein wall thickness in both methods. (6) lower stress levels for scars with longer attachment lengths. The importance and effectiveness of mechanical stress analysis in risk analysis for chronic lead management is illustrated. Overall, the localized intravascular wall stress is meaningfully higher for subclavian vs. femoral extraction with same SVC shear force. This may help explain the higher rate of SVC tears when extracting from the left subclavian approach. The individual anatomy (e.g. vascular angles) is a key factor in the resulting stress and this understanding may be critical when choosing an extraction approach and future lead design.

Keywords: Transvenous lead extraction, subclavian, femoral, finite element, mechanical vascular stress, chronic lead management, cardiac lead

1. INTRODUCTION

Approximately 400,000 CIEDs devices are implanted each year in the United States, and there are currently more than 3 million patients with implanted cardiac devices[1]. Transvenous-lead-extraction is an accepted and growing technique that has enhanced patient care. It has allowed effective treatment of many device/lead issues. Lead extraction is performed in cases of septicemia, pocket infection, pre-erosion, free-floating lead, lead related tricuspid valve insufficiency, venous occlusion, chronic pain, and vein thrombosis[2]. However, lead extraction procedures can be complex, dangerous and life-threatening with a potential for vascular tear of the SVC and thoracic vasculature. Although uncommon, SVC tears are the most common cause of lead extraction procedural deaths. Lead extraction technique requires traction applied to the lead at the point of attachment to the SVC wall to create a rail for the lead removal device to advance and track. The consequence of this traction is translation of the force to the venous structure resulting in stress within the vein wall. Transvenous lead extraction by direct traction force on implanted leads can be performed by a superior approach through the subclavian vein and superior vena cava (SVC) or an inferior approach via the femoral vein. Some physicians believe that the femoral approach results in fewer vascular tears. This study is aimed to employ Finite Element (FE) modeling in order to understand the difference in intravenous mechanical stresses between subclavian and femoral lead extraction approaches and provide better appreciation of these differences for chronic lead management.

2. MATERIALS AND METHODS

Similar to any other FE analysis the model includes three major aspects: (1) geometry (in our case veins, scars, heart, RA and RV chambers, and the lead path); (2) boundary conditions (i.e. the extraction force exerted on the lead structure and tethering force from the surrounding tissues); and (3) material properties (the veins, heart, lead, and scars). In this section, we first provide a

detailed description of our method to generate clinically relevant geometrical model using medical imaging data via image processing and CAD modeling. Next, the mechanical behavior and material properties of different components of the model as well as boundary conditions are prescribed using relevant models, experimental data, and relevant literature. Notably, due to the nature of FE no statistical analysis was performed.

2.1. Geometry:

Veins: Vascular structures of the SVC, Inferior Vena Cava (IVC) and innominate/subclavian (INN/SC) veins are represented by simple tubular geometries (Figure 1A). The diameter of SVC vein is assumed to be constant to the median SVC diameter of D = 14.74 mm (extracted from several patient specific samples using the human Magnetic Resonance Imaging (MRI) dataset library at Medtronic). These retrospective, de-identified MRI data sets are acquired under a data purchase agreement and the need for IRB is waived. It is noteworthy that this diameter is comparatively close to the value previously reported in the literature (e.g. 14.1mm±2.7mm for 108 patients by Tang *et al.*[3]). The branching angle of SVC- INN/SC veins is set to the median branching angle of θ = 120° (extracted from the same dataset). ±5° variations from the median branching angle are modeled to evaluate the effect of this geometrical factor on extraction induced vascular stress distribution. In addition, to evaluate the impact of the SVC vein thickness on mechanical vascular stress values, the SVC veins are modeled for two different vein thickness levels (δ =1.2mm and 2.4mm), extracted from the literature[4].

Fibrotic scar: The fibrotic scar tissue develops at areas of endothelial contact, as thrombus surrounds the leads and fibrosis of the thrombus occurs. This series of events results in almost complete encapsulation of the lead with a fibrin sheath within 4-5 days post implant[7].

Such adhesion occur most commonly at sites such as venous entry site, the superior vena cava and the electrode-endocardial interface[8,9]. Notably, extraction vascular tears at the venous entry site are less dangerous and trivial during the surgery. Therefore, two major lead-anatomy attachments are considered: (1) SVC fibrotic attachment of lead to the lateral wall of the SVC (at the junction with the innominate vein); and (2) attachment at the RV apex. The cross sectional shape, length and location of encapsulating fibrous scars are derived from sources such as: (1) information and pictures provided in the literature[1,5,6] (some samples are presented in Figure 1A); as well as (2) dissecting human heart specimens at the Visible Heart® laboratory of the University of Minnesota. As Figure 2b shows, the scar tissue is modeled as a 15 mm long and 1-2 mm thick struture encapsulating the lead locally. The effect of the scar size and location on vascular stress is assessed at two additional locations inferior to the innominate branch (y = 5 mm and 10 mm) and with two additional scar lengths (L = 10 mm and 5 mm).

Heart chambers (RA & RV): an algorithm is developed in Matlab® to build patient-specific geometries (Figure 1A). The algorithm works in the following order: (1) fitting ellipses (based on least-square fitting[10]) to 3-D scattered point cloud data extracted from 3-D CT images; (2) constructing smooth 3-D geometry over the ellipsoidal cross-sections; (3) 3D CAD model generating .

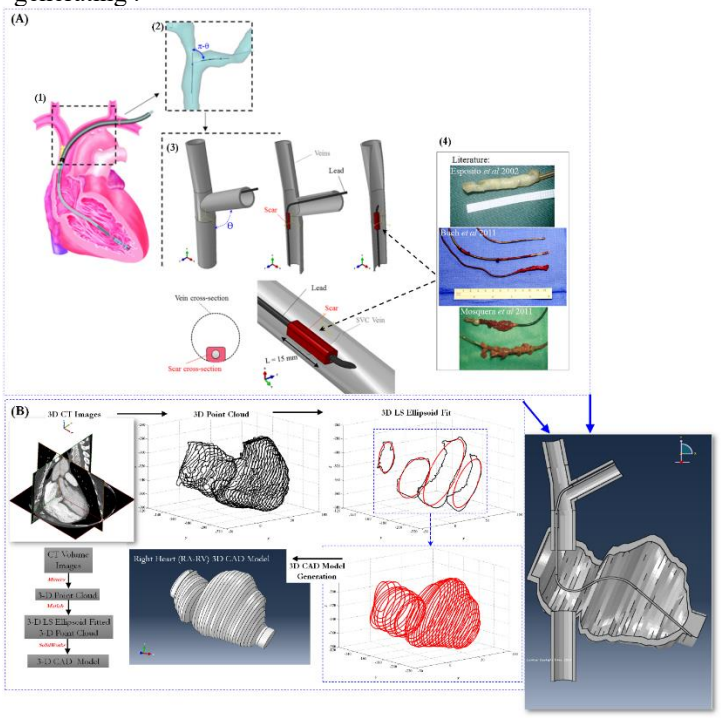

FIGURE 1: (A) (1) THE SCHEMATIC OF RA, RV, SVC, LIV AND RIV (CREDIT: BUCH ET AL. 2011), (2) THE 3-D SVC – INNOMINATE RECONSTRUCTION FROM MRI, (3) THE 3-D SIMPLIFIED CAD MODEL GENERATED USING AVERAGE BRANCHING ANGLE AND VEIN DIAMETERS ASSESSED FROM HUMAN ANATOMICAL DATA LIBRARY, AND (4) THE PROPOSED SCAR MODEL GEOMETRY BASED ON THE THREE SAMPLE PICTURES FROM THE LITERATURE SHOWING EXTRACTED LEADS WITH THE SURROUNDING FIBROUS CAPSULE (ATTACHED SCAR TISSUE). (B) THE DEMONSTRATION OF THE DEVELOPED RA-RV GEOMETRY RECONSTRUCTION ALGORITHM USING 3-D CT IMAGES.

Implanted lead shape categories: three major categories of implanted lead shapes were identified through inspection of chest X-ray images of patients with implanted cardiac leads[11]. These categories include "C-shape" for septal implant locations, "S-shape for high slack implants and "straight" for low slack implants (sample pictures of each of these categories are presented in the Supplementary Material section (see Supplementary Figure 1)). The corresponding 3-D CAD geometries of these three lead shapes are constructed and incorporated into the full 3D right heart CAD model in order to evaluate their effect on vascular stress distribution during extraction (Figure 1B).

2.2 Material properties:

The veins, the leads and myocardium tissue are modeled as hyperelastic materials. Specifically, a Mooney Rivlin model provided by Fung[12] (C_{10} = 73.825, C_{01} = 18.4563758389262 and D_1 = 0.00021818) and a Yeoh model defined based on our experimental testing data (i.e. Uniaxial, Biaxial and Planar, a sample of test results is presented in the Supplementary Figure

2) are employed for the veins and the leads, respectively. In addition, the Ogden model coefficients from Hassaballah[13]: (μ_1 = 31.9083023 psi, μ_2 = 15.9541512 psi, α_1 = 11.77 and α_2= 14.34) are used for the myocardium tissue in the FE model. Finally, the locking stylet inserted inside the lead lumen and the snare devices for femoral extraction approach are model as 304 stainless steel.

2.3. Boundary conditions:

The interactions between the blood flow with the vein walls and the heart chambers are neglected in the current FE model. Zero displacement tethers are used to the end and beginning cross sections of the vein walls, which replicates the effect of the surrounding tissues and interfaces of the vessels at the borders of the thoracic cavity.

The traction force for SVC extraction is extracted from the experimental study by Lennerz *et al* [14], where 17 physicians, experienced in transvenous lead removal, performed a lead extraction maneuver of an ICD lead on a torso phantom. The corresponding traction force for the femoral approach is then calculated using the free body diagram analysis an equal shear force within the SVC adhesion (force parallel to the vein wall axis).

3. RESULTS AND DISCUSSION

The Von-Mises stress distribution in the full models is presented for the model of straight lead shape (Figure 2A). Our computations show that the stress levels for this lead shape category is higher than the two other models (the results are not presented for brevity). The areas with highest elevated strain/stress levels (presented in red and gray colors) are seen generally near the SVC scars in both extraction approaches and for all different lead shapes. Both the maximum stress value and the extent of high stress region are both larger for subclavian approach compared to the femoral one for almost equal shear forces on the scar-vein interface. The applied traction force during subclavian extraction acts on the scar with both normal and axial (shear) components, while only the axial component is present during femoral extraction. The vascular stress resulted from the normal force component is related to the longitudinal cross section, which varies with the diameter but not the thickness. Nevertheless, the stress resulting from the shear force component is inversely related to the vein thickness ($\sim 1/\delta^2$). The ratio of the maximum vascular stress for subclavian extraction to the corresponding values of femoral approach changes from $\sigma_{Subclavian}/\sigma_{Femoral} \approx 2.3$ to 3.2 as the vascular thickness of the model is reduced from δ = 2.4mm to δ = 1.2mm. The increase in the ratios by decreasing the SVC thickness, for both full and simplified models, clearly reveals that the difference between subclavian and femoral lead extraction approaches is more substantial for patients with thinner SVC vein walls in terms of maximum vascular stresses. In addition, the maximum stress region is concentrated on the upper edge of the scar during subclavian extraction, while it is ~ uniformly distributed over the scar volume/length during the femoral extraction. This predicts that the upper region of the scar is the most prone site to SVC tears during subclavian extractions.

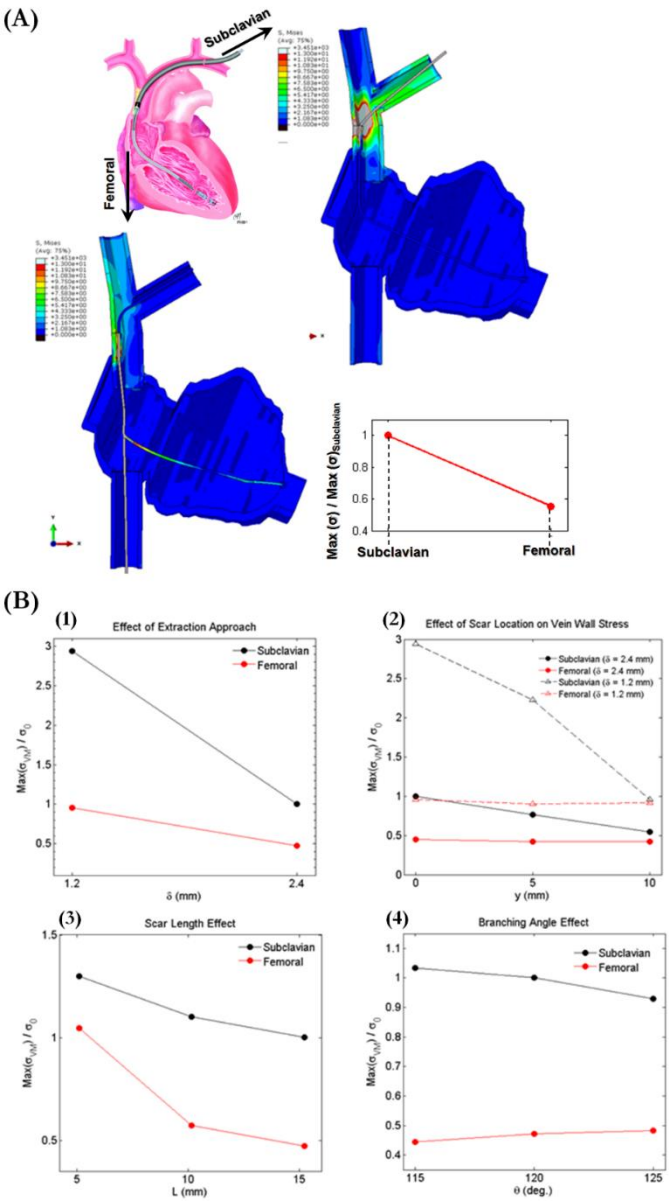

FIGURE 2: THE CONTOUR PLOTS OF THE VON-MISES STRESS DISTRIBUTION IN THE 3-D FULL MODEL WITH STRAIGHT LEAD SHAPE DURING EXTRACTION THROUGH (TOP-RIGHT) SUBCLAVIAN AND (BOTTOM-LEFT) FEMORAL. (B) THE SUMMARY OF THE EFFECTS FOR ALL GEOMETRICAL FACTORS ON MAXIMUM VASCULAR STRESS VALUES: (1) THE COMPARISON OF MAXIMUM STRESS VALUES ON THE SVC VEIN WALL DURING DIFFERENT LEAD EXTRACTION APPROACHES, (2) THE COMPARISON OF MAXIMUM STRESS VALUES ON THE SVC VEIN WALL DURING DIFFERENT LEAD EXTRACTION APPROACHES AND FOR CASES OF DIFFERENT SVC ADHESION LOCATIONS AND DIFFERENT THICKNESSES. THE STRESS VALUES ARE NORMALIZED BY MAXIMUM SVC VEIN WALL STRESS DURING SUBCLAVIAN EXTRACTION FOR THE CASE LOCATED AT Y=0 MM AND WITH Δ = 2.4 MM, (3) THE COMPARISON OF MAXIMUM STRESS VALUES ON THE SVC VEIN WALL DURING DIFFERENT LEAD EXTRACTION APPROACHES FOR FIBROSIS SCARS OF

DIFFERENT ADHESION LENGTHS. THE STRESS VALUES ARE NORMALIZED BY MAXIMUM SVC VEIN WALL STRESS DURING SUBCLAVIAN EXTRACTION FOR THE CASE WITH SCAR LENGTH OF 15 MM, AND (4) THE COMPARISON OF MAXIMUM STRESS VALUES ON THE SVC VEIN WALL DURING DIFFERENT LEAD EXTRACTION APPROACHES FOR SVC VEINS OF DIFFERENT BRANCHING ANGLES. THE STRESS VALUES ARE NORMALIZED BY MAXIMUM SVC VEIN WALL STRESS DURING SUBCLAVIAN EXTRACTION FOR THE CASE WITH BRANCHING ANGLE OF 120 DEGREES.

Unlike the stress on the SVC vein wall and scar, the maximum stress value in the myocardium for subclavian approach is smaller than femoral approach, $\sigma_{\text{Subclavian}}/\ \sigma_{\text{Femoral}} \approx 0.3$. The simulations show no significant involvement of the apex scar during extraction regardless of the approach. Specifically, the ratio of the maximum stress at the apex scar to the corresponding value for the SVC scar does not exceed 2—5% for both approaches during the stages prior to SVC-scar rupture. Therefore, we simplified the model and focused only on the upper section of the full model (see Supplementary Figure 3) for further analysis including quantitative evaluation of the effect of different scar and vein geometrical features on vein wall stress distribution. As our sanity check shows, the stress distribution around SVC vein-scar region for both simplified and full models of different extraction approaches are in a great agreement. For example, the ratio of maximum vascular stresses of subclavian to femoral extraction varies from $\sigma_{\text{Subclavian}}/\ \sigma_{\text{Femoral}} \approx 2.15$ to 3.1 as we increased the models' thickness from $\delta = 2.4$ mm to $\delta = 1.2$mm. These values are comparatively similar to the values reported earlier in this section for the full models.

As our aims were to compare these two extraction methods in terms of clinical safety and efficacy, the analysis cannot suffice to compare the maximum vein von-Mises stress values. The rupture of the lead binding scar, which is directly related to the mechanical stress level, is the desired outcome of the procedure prior to the rupture of the SVC vein wall. In other words we want to achieve $\sigma_{\text{VM-Scar}} \geq \sigma_o$ while $\sigma_{\text{VM-Vein}} < \sigma_o$, where σ_o represents the critical von-Mises stress value. Therefore, a safe and successful extraction approach leads to lower mechanical stress levels on SVC-vein wall but higher on lead-scar interface. We use we this as a comparison criterion, which can also be employed to improve the mechanical design of cardiac leads in order to manufacture devices that are easier and safer to extract compared to the previous models.

The histogram of the stress values normalized with σ_o (maximum stress on the SVC vein wall for subclavian approach) versus volume units (number of elements) are shown in Supplementary Figure 4 for all three components of the simplified models of the vein wall, the SVC scar and the lead. As it shows, the stress value within a considerable number of elements or portion of the lead binding scar volume reaches a critical value (σ_o). This indicates a similar potential for ruptures of the scar binding to the lead for both approaches. However, the stress histograms of the vein walls show significantly lower values (translates to a safer trend) for the femoral approach as compared to the subclavian. For the subclavian approach, the number of elements within the vein wall with stress values exceeding the critical value is similar to the corresponding number for the lead binding scar revealing a higher likelihood of SVC tear when applying sufficient traction to disrupt the lead binding scar.

Scar Location Effect: The FE models of subclavian extraction show that the extent of the maximum stress region, located on the upper edge of the scar, shrinks as the distance of the scar from the branching point increases. Similarly, the maximum von-Mises stress on the SVC wall reduces as this distance increases. However, the scar location has no significant effect on maximum vein wall stress for femoral extraction approach. The higher maximum stress values for the scars closer to the branching point during subclavian extraction is due to a higher ratio of the normal versus shear force component magnitudes. The highest value for this ratio coexists with the highest ratio of the maximum vein wall stress of subclavian to femoral approach in the same scar location. In addition, the difference between maximum stresses during different extraction approaches decreases as the scar distance from the branching point increases. Specifically, the ratio of the maximum vein wall stresses during subclavian and femoral approaches (Figure 2B) reduces from ~2.2 to ~1.3 as scar location distance from the branching point increases from ~ 0 mm to 10 mm for the case with 2.4 mm SVC wall thickness. This drop in the scale of the ratios is more significant for the cases with thinner SVC veins, e.g. for $\delta = 1.2$ mm. The corresponding ratio reduces from ~3.1 to ~1.1 as the distance of scar from the branching point increases from ~ 0 mm to 10 mm.

Scar Length Effect: The FE simulations are repeated for the scars located at $y = 0$ with two different attachment lengths of $L = 10$ mm and 5 mm. As the results show (Figure 2B) the maximum stress values within the SVC vein wall indicate a decreasing trend as the attachment length increases for both femoral and subclavian approaches.

Branching Angle Effect: The simulations showed no significant effect of the branching angle on maximum vein wall stress values compared to the effects of the previous geometrical factors. It is noteworthy that the range of the branching angle variations was limited to 5 degrees, and we did not observe more than 6% change in the vein wall maximum stress value as shown in Figure 2B.

CONCLUSION

4.1 Discussion: Patient specific geometry of the veins, heart (RV & RA), scars and leads are generated based on human anatomical data library, 3-D CT images and our ellipsoid fitting algorithm, literature search and dissection of implanted human heart samples and CT images, respectively.

FE modeling was employed to assess the vein wall stress distribution over the full 3-D model including veins, heart, scars and lead during lead extractions through femoral and subclavian. The results show that: (1) the areas with highest elevated strain/stress levels are seen generally in the vicinity of the SVC scars in both approaches; (2) these areas are located on the upper edge of the scar during subclavian extraction (the site most prone to SVC tears during subclavian extractions), while it is ~ uniformly distributed over the scar volume/length during the

extraction through femoral vein; (3) the vascular stress is larger for subclavian approach compared to the femoral approach; (4) the ratio of the maximum vascular stresses during subclavian extraction to the corresponding values during the femoral approach is inversely related to the SVC thickness; (5) the ratio of the maximum stress at the apex scar to the corresponding value for the SVC scar does not exceed 2—5% of the maximum stress on the SVC vein wall for both approaches, which led us to ignore the scar at the apex and develop the simplified model.

The simplified model was used to evaluate the effects of different scar and vein geometrical features on vein wall stress distribution. The summary of the results is presented in Figure 2. As this figure shows, the extent of the maximum stress regions as well as the maximum value of the von-Mises stress on the SVC wall reduces as the scar distance from the branching point increases. The scar location has no significant effect on maximum vein wall stress for femoral extraction approach. As the scar distance from the branching point increases, the difference between the maximum stresses during different extraction approaches becomes smaller, and this difference between the extraction approaches is more significant for the cases with thinner SVC veins. Regarding the scar length effect, our simulation confirms that the maximum stress values within the SVC vein wall decreases as the attachment length increases for both femoral and subclavian approaches. Finally, as our results revealed, the effect of the branching angle on maximum vein wall stress values is observed to be insignificant compared to the effects of the previous geometrical factors.

This FE-based modeling method can be used with several different lead geometries (different surface roughness structures) to evaluate probable effects of different surface textures on mechanical stress distribution of the SVC-vein wall and the SVC scar during lead extraction procedures. The results of those simulations can be employed to quantify and compare the ratio of stress levels on the SVC vein to corresponding values on the SVC scar during the extractions of the leads with different surface structures. Using the improvement criterion, i.e. achieving lower mechanical stress levels/values on the SVC-vein wall but higher on the SVC-scar during lead extractions, we can improve the lead design in order to achieve leads with easier and safer removal procedure. In addition, some surface roughness structures have been suspected to prevent/reduce the biofouling[15,16]. Therefore, this study envisions a combined computational –experimental approach of FE stress analysis and biofouling monitoring (e.g. using MRI[e.g. 17] , Ultrasound[e.g.18] or optical methods such as confocal laser microscopy[e.g.16]), to evaluate the surface roughness design effect on biofouling (scar formation, shape and properties) as well as mechanical stress during removal procedure for different roughness surface structures.

4.2 Clinical Application: The incidence of lead adherence to the SVC is uncommon[18] however the strength of the adherence is difficult to judge at this time. Critical to patient care is recognizing lead/SVC adherence and making appropriate procedural preparations. Various techniques are used to judge SVC lead adherence including intravascular Ultrasound, CT scanning and venography to evaluate if the device leads can be moved freely within the vascular space. Removal of a lead scarred to the thin SVC wall may result in a catastrophic tear and bleeding requiring emergency deployment of an occlusion balloon and thoracotomy to repair. This study is a proposal to help explain some of the clinical differences noted between superior and inferior approaches to lead extraction. Lead attachments to the SVC are uncommon and is relative to the low incidence of SVC tears

The most common approach to extraction is the superior subclavian and offers advantages of operator comfort in working from the superior position, the superior access for new lead placement, single incision procedure and the ease of removal from the right ventricle. In the unusual case of SVC lead attachment, it may be safer to remove these leads from a femoral approach

4.3 Conclusion: Here, we provide an engineering analysis of two lead extraction methods and resultant stresses applied to the vascular and myocardial walls for each approach. We have identified clinically relevant factors relating to the 2 primary approaches and how these approaches differ in SVC wall stress effects and potential complications.

Lead extraction is a critical component of lead management in CIED patients. A successful extraction program should provide multiple options of lead extraction approach that best meet the individual patient situation and safety/risk profile. Capability and experience with both the superior and the femoral approach is a necessary skill set to maximize clinical success and minimize major adverse events and vascular rupture. Future studies will likely define favored approaches to leads attached to the SVC.

The use of ultrasound and CT as imaging modalities prior to lead extraction is expanding. Through experience and technology advancement, it is expected that, preprocedural identification of SVC lead adherence will be made before the actual extraction procedure. From prior experience we believe a small but important subset of patients will be identified as having significant SVC lead attachment requiring additional care and techniques. Caution is paramount in removing attached leads from the SVC. An understanding of the vein wall stresses created during extraction is needed to further the ability to safely remove cardiac leads.

ACKNOWLEDGEMENTS

Place any acknowledgements here.

REFERENCES

[1] Buch, E., Boyle, N.G., Belott PH., 2011, ”Pacemaker and defibrillator lead extraction.” Circulation, 123:378-380.

[2] Wilkoff B.L., Love C.J., Byrd C.L., et al. 2009, “Transvenous Lead Extraction: Heart Rhythm Society Expert Consensus on Facilities, Training, Indications, and Patient Management.” This document was endorsed by the American Heart Association (AHA). Heart Rhythm. 6:1085-1104.

[3] Tang E., Restrepo M., Haggerty C.M., et al., 2014 “Geometric characterization of patient-specific total

cavopulmonary connections and its relationship to hemodynamics.” JACC Cardiovasc Imaging 7:215-224.

[4] Kholová I., Kautzner J. , 2004, “Morphology of atrial myocardial extensions into human caval veins: A postmortem study in patients with and without atrial fibrillation.”, Circulation; 110:483-488.

[5] Esposito M., Kennergren C., Holmström N., Nilsson S., Eckerdal J., Thomsen P., 2002,”Morphologic and immunohistochemical observations of tissues surrounding retrieved transvenous pacemaker leads.” J Biomed Mater Res. 63:548-558.

[6] Mosquera V.X., Pérez-Álvarez L., Ricoy-Martínez E., Mosquera-Pérez I., Castro-Beiras A., Cuenca-Castillo J.J., 2011, “Initial Experience With Excimer Laser-Assisted Pacemaker and Defibrillator Lead Extraction.”, Rev Española Cardiol (English Ed.; 64:824-827.

[7] Robboy S.J., Harthorne J.W., Leinbach R.C., Sanders C.A., Austen W.G. 1969, “Autopsy findings with permanent pervenous pacemakers.”, Circulation; 39:495-501.

[8] Smith M.C., Love C.J. 2008, “Extraction of transvenous pacing and ICD leads.” PACE - Pacing Clin Electrophysiol.; 31:736-752.

[9] Fearnot N.E., Smith H.J., Goode L.B., Byrd C.L., Wilkoff B.L., Sellers T.D., 1990, “Intravascular lead extraction using locking stylets, sheaths, and other techniques.”, Pacing and Clinical Electrophysiology; 13:1864-70.

[10] Fitzgibbon A., Pilu M., Fisher R.B., 1999, “Direct least square fitting of ellipses.” IEEE Trans Pattern Anal Mach Intell.; 21:476-480.

[11] Krahn A.D., Morissette J., Lahm R., et al. 2014, “Radiographic predictors of lead conductor fracture.”, Circ Arrhythmia Electrophysiol; 7:1070-1077.

[12] Fung Y.C., Cowin S.C., 1994,” Biomechanics: Mechanical Properties of Living Tissues”, 2nd ed. J Appl Mech.;61:1007.

[13] Hassaballah A.I., Hassan M.A., Mardi A.N., Hamdi M., 2013, “An inverse finite element method for determining the tissue compressibility of human left ventricular wall during the cardiac cycle.”, PLoS One;8(12).

[14] Lennerz, C., Pavaci, H., Grebmer, C., von Olshausen, G., Semmler, V., Buiatti, A., Reents, T., Ammar, S., Deisenhofer, I. and Kolb, C., 2014, “Forces Applied during Transvenous Implantable Cardioverter Defibrillator Lead Removal”, BioMed research international.

[15] Howell, D. and Behrends, B., 2006, “A review of surface roughness in antifouling coatings illustrating the importance of cutoff length.”, Biofouling; 22:401-410.

[16] May, R.M., Hoffman, M.G., Sogo, M.J., Parker, A.E., O’Toole, G.A., Brennan, A.B. and Reddy, S.T., 2014, “Micro-patterned surfaces reduce bacterial colonization and biofilm formation in vitro: Potential for enhancing endotracheal tube designs.”, Clinical and translational medicine; 3(1):1.

[17] Manz, B., Volke, F., Goll, D. and Horn, H., 2005, “Investigation of biofilm structure, flow patterns and detachment with magnetic resonance imaging”, Water science and technology; 52:1-6.

[18] Beaser, A., Cunnane, R., Ewulonu, N., Moss, J., Burke, M., Vatterott, P., Upadhyay, G., Broman, T., Oyenuga, O., Green, J., Ringwala, S., Nayak, H. 2015, “Degree of CIED Lead Adherence as Assessed by Intravascular Ultrasound Predicts Difficulty of Extraction. HRS Abstract Plus, Lead Extraction: Lessons Learned.

